Available online at www.sciencedirect.com
SCIENCE DIRECT®
International Journal of Heat and Mass Transfer 48 (2005) 1675–1687
International Journal of HEAT and MASS TRANSFER
www.elsevier.com/locate/ijhmt

Freeze-drying of pharmaceuticals in vials on trays: effects of drying chamber wall temperature and tray side on lyophilization performance

K.H. Gan [a], R. Bruttini [b], O.K. Crosser [a], A.I. Liapis [a,*]

[a] *Department of Chemical and Biological Engineering and Biochemical Processing Institute, University of Missouri-Rolla, Rolla, MO 65401-1230, USA*

[b] *Criofarma-Freeze Drying Equipment, Strada del Francese 97/2L, 10156 Turin, Italy*

Received 11 June 2004; received in revised form 3 December 2004

Abstract

The effects of tray side and drying chamber wall temperature on the performance of freeze-drying of pharmaceuticals in vials arranged in clusters of hexagonal arrays on trays are studied, and the results of this work indicate that it would be beneficial to operate the lyophilization process by (i) employing freeze-dryers whose trays have no tray sides, (ii) using heat input control that runs the freeze-drying process close to the melting and scorch temperature constraints during the primary and secondary drying stages, respectively, and (iii) keeping the drying chamber wall temperature slightly higher than the melting temperature constraint during the primary drying stage, while during the secondary drying stage the drying chamber wall temperature should not be significantly lower than the scorch temperature constraint. The modeling and system formulation approach presented here provide a quantitative method that can be used in the analysis, optimization and control of the lyophilization process, as well as in the design of freeze-dryers.

Keywords: Freeze drying of pharmaceuticals in vials; Lyophilization of pharmaceuticals in vials; Tray side effect; Drying chamber wall temperature effect; Drying chamber wall temperature control

1. Introduction

Freeze-drying is a very important separation process involving a moving sublimation interface and fundamental mechanisms of heat and mass transfer and its use is widespread in the fine chemicals, food, pharmaceutical, and biotechnology industries [1–6]. In this work, we are interested in the lyophilization of a product in cylindrical vials located on the surface of trays and arranged in clusters of hexagonal arrays, as shown in Fig. 1. In the freeze-dryers currently employed in industry, the trays have tray sides as shown in Fig. 1b and the movement of the sublimation interface during the primary drying stage of the lyophilization process is illustrated in Fig. 2 [3,6]. It is important to note here that the vials arranged on the tray in clusters of hexagonal arrays will have view factors differing in magnitude because of their locations on the tray. These view factors which differ among the vials could be effectively

* Corresponding author. Tel.: +1 573 341 4414/4416; fax: +1 314 965 9329.
E-mail address: ail@umr.edu (A.I. Liapis).

0017-9310/$ - see front matter © 2005 Elsevier Ltd. All rights reserved.
doi:10.1016/j.ijheatmasstransfer.2004.12.004

Nomenclature

c_{sw}	concentration of bound water (kg water/kg solid)
c^0_{sw}	initial (at $t = 0$) concentration of bound water (kg water/kg solid)
F_{lp}	view factor for radiative heat transfer from the lower heating plate (tray) to the curved side of the product in the vial (dimensionless)
$F_{tray\ side}$	view factor for radiative heat transfer from the tray side to the curved side of the product in the vial (dimensionless)
F_{up}	view factor for radiative heat transfer from upper heating plate (tray) to the top of the product in the vial (dimensionless)
$F_{wall,side}$	view factor for radiative heat transfer from the drying chamber wall to the curved side of the product in the vial (dimensionless)
$F_{wall,top}$	view factor for radiative heat transfer from the drying chamber wall to the top of the product in the vial (dimensionless)
$H(t,r)$	geometric shape (as per Fig. 2b) of the moving interface, a function of time and radial distance (m)
h_v	heat-transfer coefficient (W/K m^2)
L	length of sample (product) in vial (m)
q_I	heat flux (as per Fig. 2b) in the dried layer I at $z = 0$ (W/m^2)
q_{II}	heat flux (as per Fig. 2b) in the frozen layer II at $z = L + \psi$ (W/m^2)
q_{III}	heat flux (as per Fig. 2b) in the side of the vial at $r = R + \delta$ (W/m^2)
r	space coordinate of radial distance (m)
R	radius of vial (m)
R_{frozen}	radial extent of frozen layer, as per Fig. 2d (m)
t	time (s)
t_a	t when first $H(t,R) = L$, as per Fig. 2d (s)
t_b	t when first $H(t,0) = L$, as per Fig. 2d (s)
T_{glass}	temperature of vial glass (K)
T_{lp}	temperature of lower heating plate (tray) (K)
T_m	melting temperature of frozen layer II (K)
T_{scor}	scorch temperature of dried layer I (K)
$T_{tray\ side}$	temperature of tray side (K)
T_{up}	temperature of upper heating plate (tray) (K)
T_{wall}	temperature of wall of drying chamber (K)
T_I	temperature in dried layer I (K)
T_{II}	temperature in frozen layer II (K)
z	space coordinate of distance along the length of the vial (m)

Greek symbols

β	angle between tangent to interface at $r = R$ and horizontal, as defined in Eq. (4) (deg)
δ	thickness of the glass wall of the side of the vial (m)
θ	thickness of gas gap (m)
σ	Stefan–Boltzmann constant (W/m^2 K^4)
χ	thickness of the glass at the bottom of the vial (m)
ψ	sum of χ and θ ($\psi = \chi + \theta$) (m)

accommodated [6] by five distinct sets of vials on the tray as shown in Fig. 1b, whose view factors could be considered as representing an effective medium approximation [6–10] among the differing view factors of the vials on the tray. The vials on the five different characteristic locations on the tray shown in Fig. 1b can be associated with vials receiving distinctively different heat inputs q_I and q_{III} (Fig. 2b). These vials are designated as (i) center vials, (ii) side vials of type 1s, (iii) side vials of type 2s, (iv) side vials of type 3s, and (v) corner vials, and their respective locations on a tray are shown in Fig. 1b. In practice, clusters of vials in hexagonal arrays on a tray are preferred over square arrays because more vials of the same size can fit on a given surface area of a tray when the vials are arranged in clusters of hexagonal arrays. Sheehan and Liapis [3] and Gan et al. [6] have shown that heat input control that runs the lyophilization process close to the melting and scorch temperature constraints yields (1) faster drying times, and (2) more uniform distributions of temperature and bound water at the end of the secondary drying stage; this result provides a more stable product during storage.

Kobayashi et al. [2] studied the inter-vial variance of the sublimation rate during the primary drying stage by constructing a laboratory-scale freeze-dryer whose drying chamber wall temperature could be controlled. They found [2] that by controlling the drying chamber wall temperature the inter-vial variance of the sublimation rate as well as the duration of the primary drying stage could be decreased; Kobayashi et al. [2] used a heat input policy that did not run the lyophilization process close to the temperature constraints. Gan et al. [12] and Gan [14] have shown that during the primary and secondary drying stages heat input control that runs the freeze-drying process at the temperature constraints has a much more significant effect in reducing the inter-vial variance of the sublimation rate and

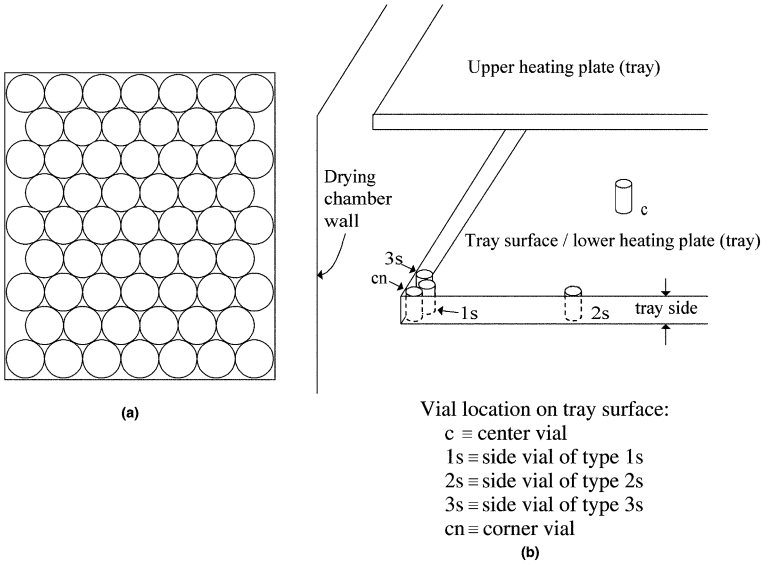

Fig. 1. (a) Clusters of hexagonal arrays of vials on a tray; (b) characteristic locations of vials on a tray surface when the vials on the tray are arranged in clusters of hexagonal arrays.

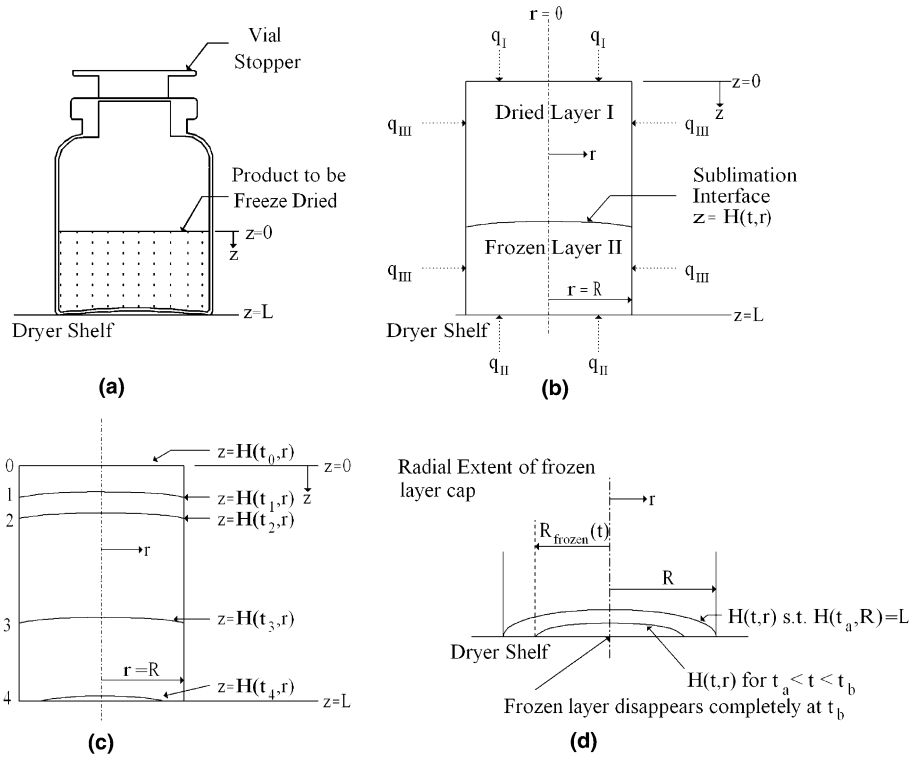

Fig. 2. (a) Cylindrical vial with stopper used in the lyophilization of pharmaceutical products; (b) diagram of a material being freeze-dried in a vial; (c) depiction of the observed movement of the sublimation interface in the material in a vial; and (d) radially distributed disappearance of frozen layer.

the drying time than in the case of a system that employs drying chamber wall temperature control and a heat input policy that runs the freeze-drying process below the temperature constraints. While control of the drying chamber wall temperature would be required [11–13] during the freezing stage of the lyophilization process, Gan et al. [12] have shown that the extra expense that would be required to control the drying chamber wall temperature during the primary and secondary drying stages of the freeze-drying process employing trays with tray sides would provide a very small reduction in the drying time and the inter-vial variance of the sublimation rate as long as heat input control during the primary and secondary drying stages runs the lyophilization process at the temperature constraints [3,6,12].

Furthermore, Gan et al. [12] and Gan [14] have found that when heat input control runs the lyophilization process at the temperature constraints, the drying time decreases as the height of the tray side (Fig. 1b) decreases. This finding [12,14] also led us to study the dynamic behavior of a freeze-drying system where the trays have no tray sides, and in this work the results of this study are reported.

2. System formulation and modeling

The lyophilization process in this work is conducted with cylindrical vials (Fig. 2a) arranged in clusters of hexagonal arrays (Fig. 1) being dried simultaneously on the tray. It is important to indicate here that on a tray that measures 0.8 m × 0.8 m, 2822 vials having each a diameter of 0.016 m [15] can be placed on this tray; center vials make up 92.56% (2612 vials) of the total number of vials on the tray, 1s vials make up 1.99% (56 vials) of the total number of vials on the tray, 2s vials represent 3.40% (96 vials) of the total number of 2822 vials, 3s vials represent 1.91% (54 vials) of the total number of 2822 vials, and there are four corner vials on the tray that represent 0.14 % of the total number of vials.

The rigorous unsteady state and spatially multidimensional model of Sheehan and Liapis [3] is used to study the dynamic performance of the lyophilization process in cylindrical vials and to determine the effects of the tray side on the overall drying time and the distributions of the temperature and concentration of bound water in the product at the end of the freeze-drying process; these distributions affect the stability of the product during storage. The heat inputs q_{I}, q_{II}, and q_{III} to the product (Fig. 2b) employed in the model of Sheehan and Liapis [3] when the cylindrical vials are arranged in clusters of hexagonal arrays on the tray (Fig. 1), are determined from Eqs. (1)–(3):

$$q_{\mathrm{I}} = q_{\mathrm{I}}|_{z=0} = \sigma F_{\mathrm{up}}\left(T_{\mathrm{up}}^4 - T_{\mathrm{I}}^4|_{z=0}\right) + \sigma F_{\mathrm{wall,top}}\left(T_{\mathrm{wall}}^4 - T_{\mathrm{I}}^4|_{z=0}\right) \quad (1)$$

$$q_{\mathrm{II}} = q_{\mathrm{II}}|_{z=L+\psi} = h_v\left(T_{\mathrm{lp}} - T_{\mathrm{glass}}\big|_{z=L+\chi}\right) \quad (2)$$

$$q_{\mathrm{III}} = q_{\mathrm{III}}|_{r=R+\delta} = \sigma F_{\mathrm{lp}}\left(T_{\mathrm{lp}}^4 - T_{\mathrm{glass}}^4\Big|_{r=R+\delta}\right) + \sigma F_{\mathrm{tray\ side}}\left(T_{\mathrm{tray\ side}}^4 - T_{\mathrm{glass}}^4\Big|_{r=R+\delta}\right) + \sigma F_{\mathrm{wall,side}}\left(T_{\mathrm{wall}}^4 - T_{\mathrm{glass}}^4\Big|_{r=R+\delta}\right) \quad (3)$$

The variable z is the longitudinal distance measured from the top surface of the product in the vial (Fig. 2b). The variable ψ is the sum of the thickness of the glass at the bottom of the vial, χ, and the thickness of the gas gap, $\theta(\psi = \chi + \theta)$. The first term in Eq. (3) is the heat input originating from the inter-vial area on the surface of the tray where the vial is located, the second term represents the heat input from the tray side, and the third term quantifies the heat input originating from the drying chamber wall. From Eq. (2), one sees that the amount of heat input into the bottom of the vial for each vial, as quantified by q_{II}, is the same for a vial placed in different locations on the tray. The amount of heat input into the top surface of the vial, q_{I}, differs for a vial placed in different locations on the tray due to the differing view factors of each vial to the upper heating plate, F_{up}, and to the drying chamber wall, $F_{\mathrm{wall,top}}$. Similarly, the amount of heat input into the curved side of the vial, q_{III}, differs for a vial in different locations on the tray due to the differing view factor of each vial to the lower heating plate, F_{lp}, the differing view factor of each vial to the tray side, $F_{\mathrm{tray\ side}}$, and to the drying chamber wall, $F_{\mathrm{wall,side}}$. In the case where the height of the tray side is equal to the height of the product in the vial, the variable $F_{\mathrm{wall,side}}$ is set equal to zero as the curved side of the vial does not "see" the drying chamber wall; in the case where the height of the tray side is equal to zero, the variable $F_{\mathrm{tray\ side}}$ is set equal to zero as the curved side of the vial does not "see" the tray side. For a tray side whose height is greater or smaller than the height of the product in the vial, Eqs. (1) and (3) can be easily modified to account for the different view factors. For example, in the case where the height of the tray side is greater than the height of the product in the vial, an additional view factor from the top surface of the product to the tray side, $F_{\mathrm{tray\ side,top}}$, is added to Eq. (1), as shown in Gan [14]. In the case where the height of the tray side is smaller than the height of the product in the vial, Eq. (3) would be modified to account

for two different regions along the curved side of the vial (above and below the tray side, respectively) that have distinctively different view factors to the tray side, $F_{\text{tray side}}$, and to the drying chamber wall, $F_{\text{wall,side}}$, as shown in Gan [14].

The product in the vials is taken at time $t \leqslant 0$ (before the start of the primary drying stage of the lyophilization process) to be a frozen solution of skim milk; this product was selected because it could be considered as a complex pharmaceutical product in the sense that it contains enzymes and proteins [3,16]. The height, L, and radius, R, of the product in the vial are taken to be equal to 0.016 m and 0.007 m, respectively, the thickness of the glass at the bottom of the vial was 0.0007 m and the radius of the stopper was 0.0062 m; these dimensions are representative of the international standard [15] used for lyophilization in vials. A tray of dimensions of $0.8\text{ m} \times 0.8\text{ m}$ was considered and in determining the influence of the tray side on the process two cases were studied: (i) a tray with tray side and (ii) a tray without tray side. In case (i), the height of the tray side is taken to be equal to 0.0174 m and this height is equal to the sum of the height, L, of the product in the vial and the thickness, χ, of the glass of the vial (0.0007 m) and the thickness, θ, of the gas gap (0.0007 m) at the bottom of the vial [15]. In case (ii), the height of the tray side is taken to be equal to 0 m. The values of the view factors and heat transfer coefficient employed in Eqs. (1)–(3) for the systems studied in this work are shown in Table 1 while the detailed calculations for determining these values can be found in Gan [14]; also in Gan [14] one can find the expressions for determining the values of the view factors when the height of the tray side is larger or smaller than the height of the product in the vial. Furthermore, the distance between the drying chamber wall and the side of the tray was 0.075 m while the distance between the upper heating plate (tray) and the top of the product in the vial was equal to 0.0986 m. The melting, T_{m}, and scorch, T_{scor}, temperatures of the product are 263.15 K and 313.15 K, respectively, and the value of the drying chamber wall temperature, T_{wall}, was kept at a constant value. The values of all the other parameters of the lyophilization system studied in this work, are given in Table 1 of the work of Sheehan and Liapis [3].

3. Results and discussion

In this work, a heat input control policy is used that runs the process (i) close to the melting temperature constraint during the primary drying stage where the frozen water is removed by sublimation, and (ii) close to the scorch temperature constraint during the secondary drying stage where bound (sorbed) water is removed by desorption [3,5,12,14], for all vials being arranged in clusters of hexagonal arrays and dried simultaneously on the tray. During the primary drying stage, this heat input control policy was achieved by monitoring the product temperature in each type of vial (Fig. 1b) and controlling the heat input so not to melt the product first in the most vulnerable vial (the vial that receives the highest amount of heat input); after the primary drying stage of the most vulnerable vial was completed, the heat input was controlled so not to melt the product in the next most vulnerable vial, and this sequence is repeated until all the vials on the tray have completed their primary drying stages. Because there will be some vials on the tray that have completed their primary drying stage and have started their secondary drying stage while some other vials are still in their primary drying stage, the heating plate temperature, T_{lp}, in Fig. 3 could be increased, decreased, and increased again to satisfy the

Table 1
Values of the view factors and heat transfer coefficient used in Eqs. (1)–(3) for cases (a)–(c)

Parameters in Eqs. (1)–(3)		Location of vial				
		Center	Side			Corner
			1s	2s	3s	
Case (a)	F_{up}	0.86	0.272	0.444	0.281	0.209
	$F_{\text{wall,top}}$	0.06	0.648	0.476	0.639	0.711
	F_{lp}	0.0203	0.04847	0.02344	0.0501	0.035
	$F_{\text{tray side}}$	0	0.2722	0.5	0.5	0.75
	$F_{\text{wall,side}}$	0	0	0	0	0
	h_v (W/m^2 K)	30.0	30.0	30.0	30.0	30.0
Cases (b) and (c)	F_{up}	0.86	0.272	0.444	0.281	0.209
	$F_{\text{wall,top}}$	0.06	0.648	0.476	0.639	0.711
	F_{lp}	0.0203	0.04847	0.02344	0.0501	0.035
	$F_{\text{tray side}}$	0	0	0	0	0
	$F_{\text{wall,side}}$	0	0.2722	0.5	0.5	0.75
	h_v (W/m^2 K)	30.0	30.0	30.0	30.0	30.0

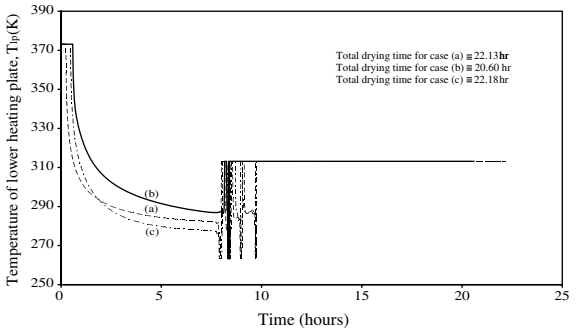

Fig. 3. Program of the temperature, T_{lp}, of the lower heating plate (tray) for cases (a)–(c).

temperature constraints and at the same time run the process as close as possible to the melting and scorch temperature constraints. When the least vulnerable vial has completed its primary drying stage, the heating plate temperature, T_{lp}, is raised to the value of the scorch temperature of the product in the vials until the total amount of bound water remaining at the end of the secondary drying stage in the product in the center vial, which represents more than 90% of all vials on the tray, reaches 3% [3,4,6,12] of the total amount of bound water present at the beginning of the primary drying stage in the product in the vial, whereupon the lyophilization process is terminated. In Fig. 3, the variation of the temperature, T_{lp}, of the heating plate (that is, the variation of the temperature of the tray) with respect to time is presented for the cases where (a) the height of the tray side is equal to the height of the product and $T_{wall} = 263.15$ K for all times, (b) the height of the tray side is equal to zero and $T_{wall} = 263.15$ K for all times, and (c) the height of the tray side is equal to zero and $T_{wall} = 293.15$ K for all times. The values of the view factors and heat transfer coefficient used in Eqs. (1)–(3) for cases (a)–(c) are reported in Table 1 while the detailed calculations for determining these values can be found in Gan [14]. During the primary drying stage, the heat input to the curved side of the corner and side vials is largest in case (a) due to the presence of the tray side, which is maintained at 373.15 K initially and which represents the highest temperature achieved by the equipment. Thus, in case (a), the corner vial becomes the most vulnerable vial on the tray and the large side heat input, q_{III}, causes the melting temperature constraint to be reached first in the corner vial in case (a), as shown in Fig. 3. In case (b), the removal of the tray side and the low drying chamber wall temperature at 263.15 K reduces by a significant amount the magnitude of the heat transferred to the side and corner vials. Thus, in case (b), the center vial receives more heat compared to the side and corner vials and is the most vulnerable vial. Because of the lower heat input into the curved side of the center vial, the melting temperature constraint is reached at a much later time after the start of the primary drying stage in the center vial in case (b), when the temperature, T_{lp}, of the lower heating plate is first reduced, as shown in Fig. 3. In case (c), even with the removal of the tray side, the drying chamber wall temperature is being maintained at 293.15 K and this means that a larger heat input arrives at the curved sides of the side and corner vials from the drying chamber wall. Thus, in case (c), the corner vial is the most vulnerable vial. The temperature, T_{lp}, of the lower heating plate (tray) in the case where the tray side is removed and the drying chamber wall temperature is kept at 263.15 K (case (b)) remains the highest among the three cases shown in Fig. 3 during the primary drying stage, because the heat input at the curved side of the vials, q_{III}, in case (b) is substantially smaller in magnitude than the value of q_{III} in cases (a) and (c). This allows a higher operational temperature, T_{lp}, of the lower heating plate (tray) to be employed in order to maintain the product temperature in the center vial close to its melting temperature constraint. In Fig. 3, the temperature, T_{lp}, of the lower heating plate (tray) in case (c) has to be reduced below the temperature, T_{lp}, of the lower heating plate (tray) in case (a) some time after the start of the primary drying stage, because the higher drying chamber wall temperature maintained in case (c), compared to the temperature of the tray side in case (a) whose temperature varies as shown in Fig. 3, supplies more heat to the curved side of the corner vial than in case (a) and, thus, the heat that needs to be supplied from the lower heating plate (tray) is lower in case (c). It is also observed from Fig. 3 that the temperature, T_{lp}, of the lower heating plate in case (b) is decreased, increased, and decreased fewer times and this makes the duration of the primary drying stage to be shorter in case (b) than in cases (a) and (c).

In Table 2 the total drying times as well as the drying times of the primary drying, changeover, and secondary drying stages, for cases (a)–(c) are presented. From Table 2 one can determine that the total drying time in the case where the tray side is removed from the tray is 6.9% shorter relative to the total drying time in the case where the height of the tray side is equal to the height of the product. This is because in the case where the tray side is removed and heat loss from the side and corner vials to the drying chamber wall occurs, as in case (b), the temperature, T_{lp}, of the lower heating plate (tray) required to dry the product in the center vial close to the melting temperature constraint would be able to satisfy the temperature constraint of the product in the side and corner vials and thus, could dry the product in the side and corner vials on the tray sufficiently close to their melting temperature constraint, and this shortens the overall drying time. The data in Table 2 also show that the primary drying time for the center vial placed on the tray without tray side, which represents

Table 2
Primary, changeover, secondary, and total drying times for the vials in cases (a)–(c)

	Drying times			
	Primary	Changeover	Secondary	Total
Case (a)				
T_{wall} = 263.15 K for all times				
Center	9.69	0.004	12.44	22.13
1s	8.99	0.051	13.09	22.13
2s	8.40	0.075	13.66	22.13
3s	8.37	0.076	13.69	22.13
Corner	7.87	0.099	14.16	22.13
Case (b)				
T_{wall} = 263.15 K for all times				
Center	8.15	0.005	12.45	20.60
1s	8.39	0.011	12.20	20.60
2s	8.33	0.007	12.26	20.60
3s	8.33	0.011	12.26	20.60
Corner	8.38	0.012	12.21	20.60
Case (c)				
T_{wall} = 293.15 K for all times				
Center	9.74	0.004	12.44	22.18
1s	8.91	0.053	13.22	22.18
2s	8.41	0.084	13.69	22.18
3s	8.37	0.073	13.74	22.18
Corner	7.89	0.148	14.14	22.18

more than 90% of all vials on the tray, has decreased by 15.9%, relative to the primary drying time for the center vial placed on the tray with tray side whose height is equal to that of the product. In case (a) where the tray side is present and the drying chamber wall temperature is at 263.15 K for all times as well as in case (c) where the tray side is removed and the drying chamber wall temperature is at 293.15 K for all times, the temperature, T_{lp}, of the lower heating plate (tray) is based on the melting temperature constraint in the corner vial. Thus, in these two cases, the primary drying time for the corner vials is the shortest among all the vials on the tray, as shown in Table 2. Furthermore, the corner vials in cases (a) and (c) receive significant amounts of heat from the tray side and the drying chamber wall, respectively, and, thus, the temperature, T_{lp}, of the lower heating plate (tray) is much lower than in case (b) and does not dry the product in the overwhelming majority of the vials (center vials) on the tray sufficiently close to their melting temperature constraint. This results in longer overall drying times for cases (a) and (c) as observed by comparing the results in Table 2.

The time quoted for "changeover" in Table 2 gives the drying time taken up by the phenomenon where there is a time period when primary and secondary drying coexist [3,6,12–14] within the vial, and, thus, the time difference $t_b - t_a$ (Fig. 2d) provides the value of the changeover time. The data in Table 2 indicate that the changeover time is significantly smaller in case (b) when compared with cases (a) and (c). This result would suggest that the curvature of the moving sublimation interface in the vials of case (b) would be substantially smaller than that of cases (a) and (c). This is found to be the case by comparing the values of the angle β in Table 3 and the shape of the moving sublimation interface in Fig. 4a–c. The value of the tangent of the angle β is obtained from Eq. (4)

$$\tan\beta = \left.\frac{\partial H(t,r)}{\partial r}\right|_{r=R} \tag{4}$$

where β is the angle between the horizontal and a tangent to the interface surface at $r = R$; thus, the angle β gives a quantitative measure of the curvature of the interface. The value of the angle β is determined [3,6,12,14] from the generated form of $H(t,r)$ using Eq. (4). From Table 3, it can be observed that for case (b) the values of the angle β in the center vials are very small while the values of the angle β for the side and corner vials are significantly smaller than the values of the angle β for the center, side, and corner vials of cases (a) and (c). In Fig. 4a–c, the profile of the moving sublimation interface, $H(t,r)$, along r and its position along z at various times during the primary drying stage is presented in the different types of vials on the tray, for cases (a)–(c), respectively. All z-axes are drawn to the same scale and, thus, the curvature of the interface as it proceeds in time for the three cases can be compared. It is noted here that in Fig. 4a–c, the r and z-axes have different scales and, thus, the values of the angle β in Table 3 are not faithfully represented in these figures. The

Table 3
Values of the angle β (in degrees) at different times during the primary drying stage for cases (a)–(c)

At time (h)	Location of vial				
	Center	Side			Corner
		1s	2s	3s	
Case (a)					
2.0	0.06	0.95	1.50	1.57	2.17
4.0	0.07	0.99	1.53	1.60	2.18
6.0	0.07	1.01	1.54	1.62	2.19
7.5	0.07	1.02	1.56	1.64	2.21
Case (b)					
2.0	0.09	0.33	0.29	0.41	0.45
4.0	0.09	0.29	0.24	0.35	0.38
6.0	0.08	0.26	0.20	0.30	0.31
7.5	0.09	0.24	0.17	0.27	0.27
Case (c)					
2.0	0.06	0.93	1.46	1.52	2.08
4.0	0.06	1.19	1.92	1.97	2.70
6.0	0.06	1.36	2.20	2.25	3.09
7.5	0.06	1.45	2.35	2.40	3.31

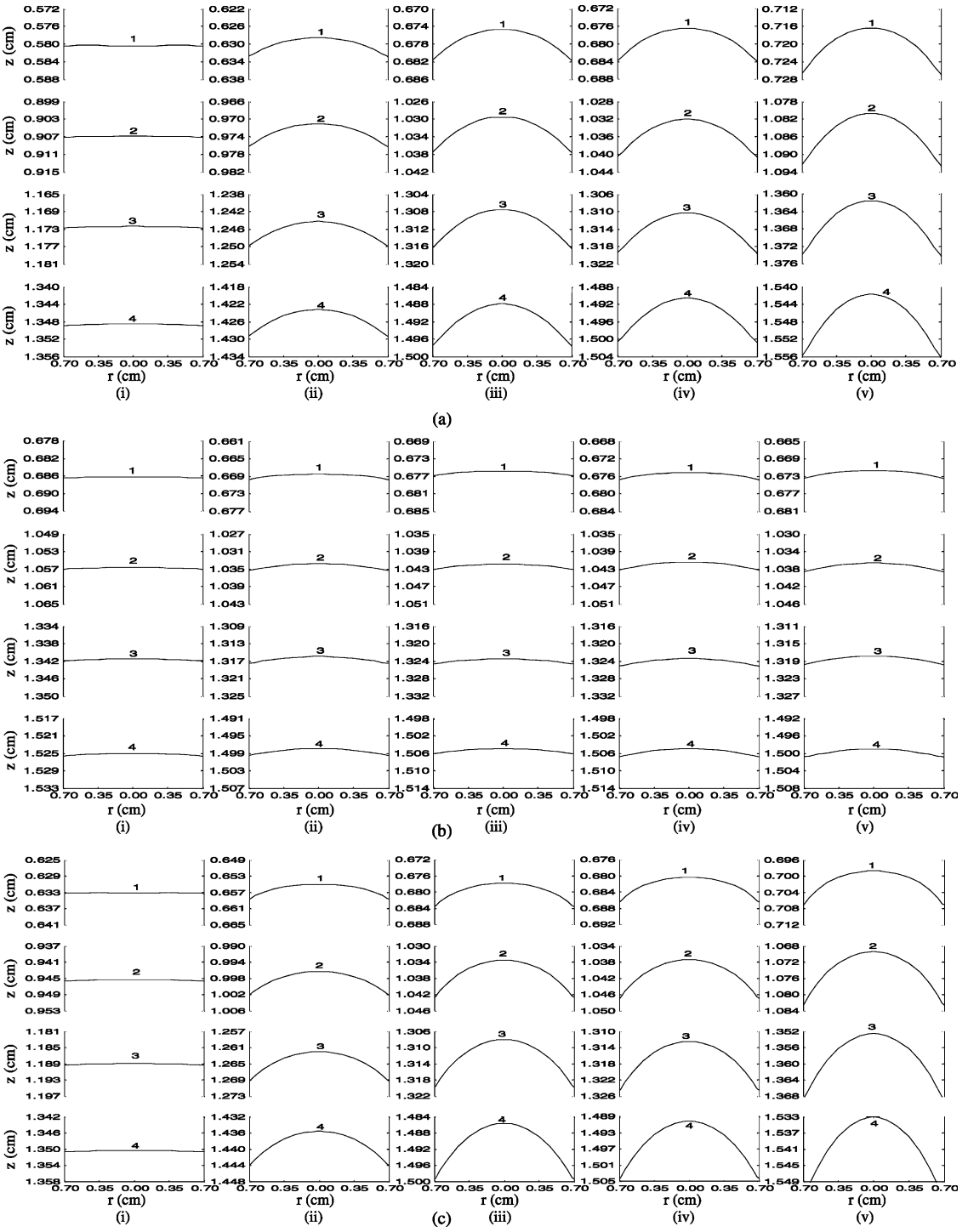

Fig. 4. Locus of moving sublimation interface, $H(t,r)$, for cases (a)–(c) and for the (i) center, (ii) 1s side, (iii) 2s side, (iv) 3s side, and (v) corner vials; $1 \equiv 2$ h, $2 \equiv 4$ h, $3 \equiv 6$ h, and $4 \equiv 7.5$ h. Fig. 4a–c represent the results for cases (a)–(c), respectively.

progress of the moving interface is greatest for the product in the center vial in case (b), followed by the 3s vial, the 2s vial, the corner vial, and then by the 1s vial. In cases (a) and (c), the progress of the interface is greatest

for the product in the corner vial, followed by the 3s vial, the 2s vial, the 1s vial, and then by the center vial. The largest curvature of the interface occurs for all times in the product of the corner vials and the lowest in the product of the center vials. It is observed that in Fig. 4b, the velocity of the interface proceeding down the product does not vary as much among vials placed at different locations on the tray, as shown by the positions of the moving interface on the z-axis at the same time, t, for the different types of vials, when the tray side is removed and the drying chamber wall temperature is at 263.15 K (case (b)). It has been shown [3,6,12,14] that as the curvature of the moving sublimation interface becomes smaller, then the distribution of the concentration of bound water at the end of the secondary drying stage becomes more uniform, and this result is desirable for the long-term stability of the pharmaceutical product.

In Fig. 5a–c, the temperature distribution in the product at the end of the secondary drying stage is presented for cases (a)–(c), respectively. In all contour plots presenting temperature distributions in the product in the vial, the solid and dotted lines are isotherms; the dotted lines represent equal graduations in temperature between the temperature values quoted on the solid lines. The results in Fig. 5a–c show that the temperature gradient in the longitudinal direction is smallest in the product in the vials of case (a), and the temperature gradient in the longitudinal direction in the product in the vials of case (c) is smaller than that of case (b). The results in Fig. 5a–c indicate that the temperature distribution is most uniform in the center vial for all cases (a)–(c), and it is worth mentioning again here that more than 90% of all vials on the tray are center vials. The results in Fig. 5a–c indicate that the temperature distribution in the product in the vial at the end of the lyophilization process is affected by the position of the vial on the tray and the magnitude of the drying chamber wall temperature. In Fig. 6a–c, the distribution of the concentration of bound water in the product in the vial at the end of the lyophilization process is presented for cases (a)–(c), respectively. In all contour plots presenting the distribution of the concentration of bound water in the product, the solid and dotted lines are isoconcentrations; the dotted lines represent equal graduations in concentration of bound water between the concentration of bound water values quoted on the solid lines. The results in Table 3 and Fig. 4a–c together with the results in Fig. 6a–c clearly show that the degree of relative uniformity in the distribution of the concentration of bound water in the product in the vials at the end of the lyophilization process is increased when the curvature of the moving interface (or the value of the angle β) is decreased. It is noted here that the most uniform distribution of the concentration of bound water, exhibited by the smallest gradients in the distribution of the concentration of bound water both in the longitudinal and radial directions, is obtained for case (b) where the tray has no tray side and the drying chamber wall temperature, T_{wall}, is kept at 263.15 K at all times. It should be noted here that the initial concentration, c^0_{sw}, of bound water everywhere in the product at the start of the primary drying stage was equal to 0.6415 kg water/kg solid.

The value of the percentage of bound water remaining in the product in the vials at the end of the lyophilization process relative to the amount of bound water in the vials at the start of the primary drying stage has been shown [4] to be an important parameter for maintaining product stability and quality during storage of the product. The values comparing the percentage of bound water remaining in the product in the vials at the end of the lyophilization process relative to the amount of bound water in the vials at the start of the primary drying stage for cases (a)–(c) are presented in Table 4. The data in Table 4 clearly show that in case (b) where the tray side is removed and the drying chamber wall temperature is kept at 263.15 K at all times, the total amount of bound water remaining in the product in the side and corner vials is much closer to the total amount of bound water remaining in the product in the center vials at the end of the lyophilization process, when compared with the differences in the total amount of bound water remaining in the product in the side, corner, and center vials of cases (a) and (c). This indicates that a larger portion of the vials on the tray in case (b) will have an amount of bound water remaining in the product at the end of the lyophilization process that is closer to the desirable amount (3%) necessary for the stability of the product during storage [4]. This is also supported by the results in Fig. 6a–c where for case (b) the vials located at different locations on the tray are found to have concentrations of bound water that are closer in magnitude to each other than for cases (a) and (c).

The inter-vial dynamic water loss for cases (a)–(c) is presented in Figs. 7–9, respectively. By comparing the results in Figs. 7–9, it can be observed that the water loss in vials located at different positions on the tray has the highest degree of uniformity in case (b), as shown by the overlapping curves in Fig. 8; it is also important to note again here that case (b) has the shortest overall drying time, as shown previously in Table 2. In cases (a) and (c), water loss is highest in the corner vial, followed by the 3s vial, the 2s vial, the 1s vial, and is lowest in the center vial. In both cases (a) and (c), the water loss in the 2s vial and the 3s vial is very similar, as shown in Figs. 7 and 9. In case (a), this is because both of these vials have very similar view factors from their curved sides to the tray side, $F_{\text{tray side}}$, as reported in Table 1; it should be noted again here that in case (a) the lower heating plate and the tray side have the same temperature during the lyophilization process. In case (c), the similarity in the water loss with time in the 2s and 3s

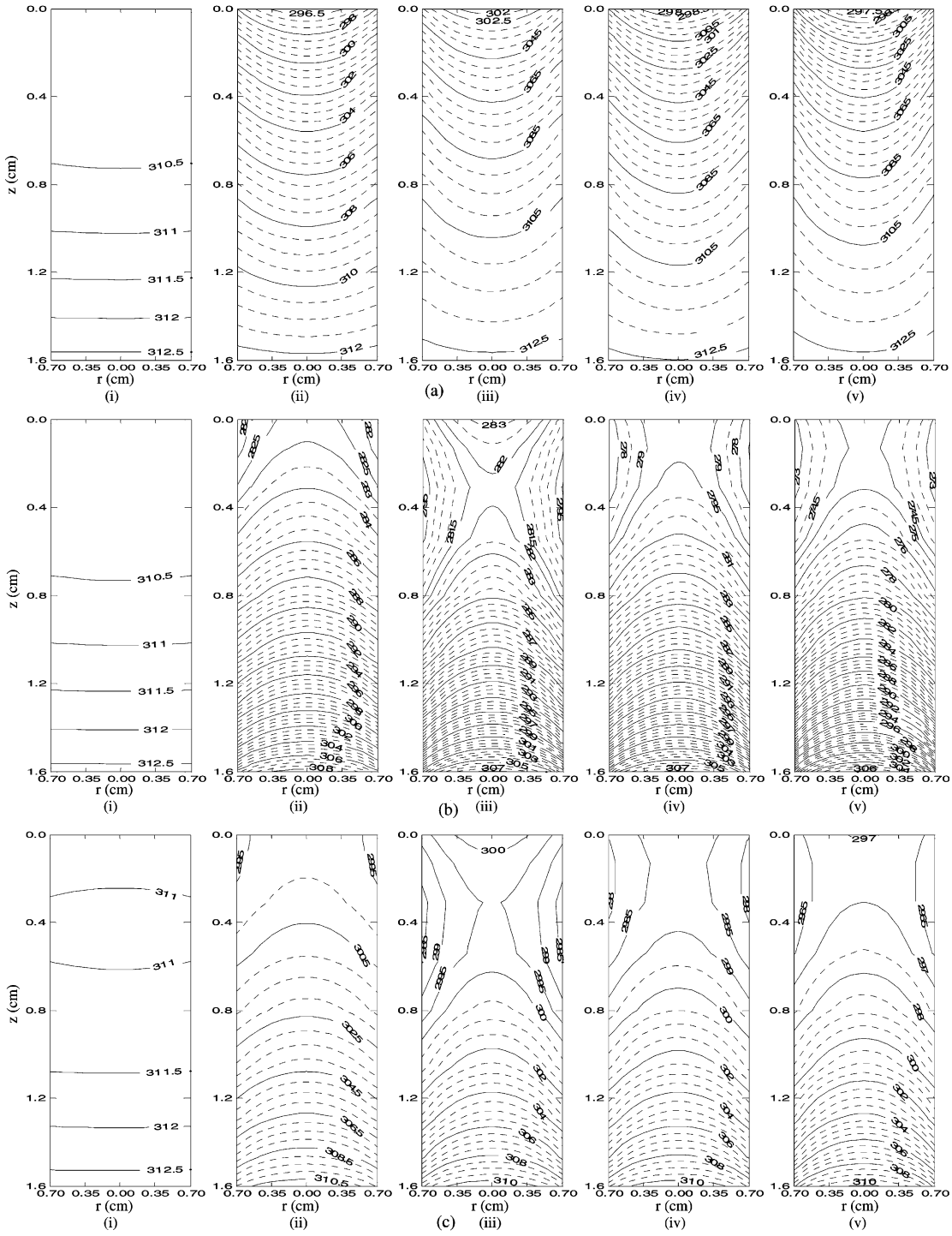

Fig. 5. Temperature distribution in the product at the end of the lyophilization process for case (a) (time t = 22.13 h), case (b) (time t = 20.60 h), and case (c) (time t = 22.18 h), and for the (i) center, (ii) 1s side, (iii) 2s side, (iv) 3s side, and (v) corner vials. Fig. 5a–c represent the results for cases (a)–(c), respectively.

vials is due to the similarity in the view factors from their curved sides to the drying chamber wall, $F_{\text{wall,side}}$, as shown in Table 1. Finally, while the difference in the overall drying times between cases (a) and (c) is insignif-

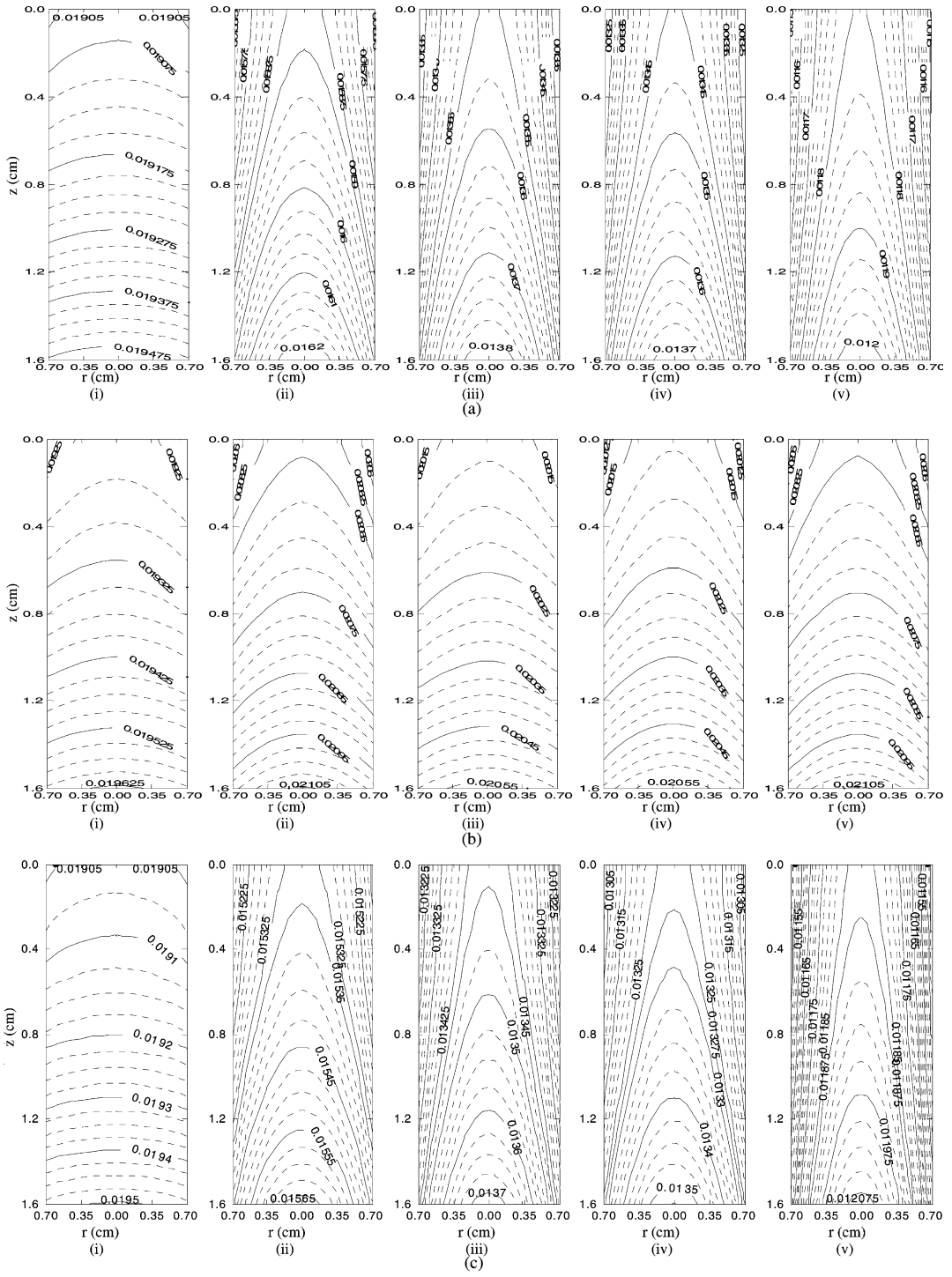

Fig. 6. Distribution of the concentration of bound water, c_{sw} (kg water/kg solid), in the product at the end of the lyophilization process for case (a) (time t = 22.13 h), case (b) (time t = 20.60 h), and case (c) (time t = 22.18 h), and for the (i) center, (ii) 1s side, (iii) 2s side, (iv) 3s side, and (v) corner vials. Fig. 6a–c represent the results for cases (a)–(c), respectively.

icant (Table 2), it can be observed by comparing Figs. 7 and 9 that the differences in inter-vial water losses are smaller in case (c) where there is no tray side than in case (a) where there is a tray side. It is also important to

Table 4
Percentage of bound water remaining in the product in the vials at the end of the lyophilization process relative to the amount of bound water in the product in the vials at the start of the primary drying stage for cases (a)–(c)

	Center vials	Side vials			Corner vials
		1s	2s	3s	
Case (a) Tray with tray side and T_{wall} = 263.15 K Percentage (%)	3.00	2.47	2.10	2.08	1.82
Case (b) Tray without tray side and T_{wall} = 263.15 K Percentage (%)	3.00	3.21	3.16	3.15	3.20
Case (c) Tray without tray side and T_{wall} = 293.15 K Percentage (%)	3.00	2.39	2.08	2.05	1.81

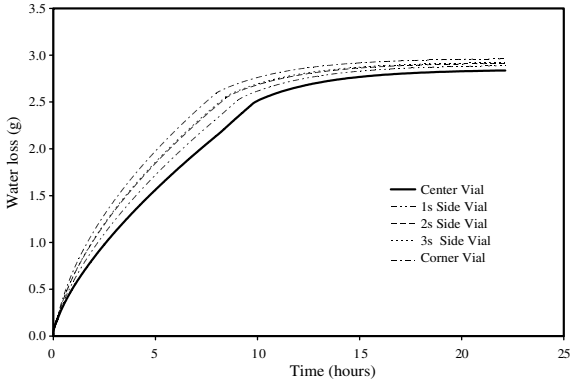

Fig. 7. Water loss as a function of time for the vials of case (a).

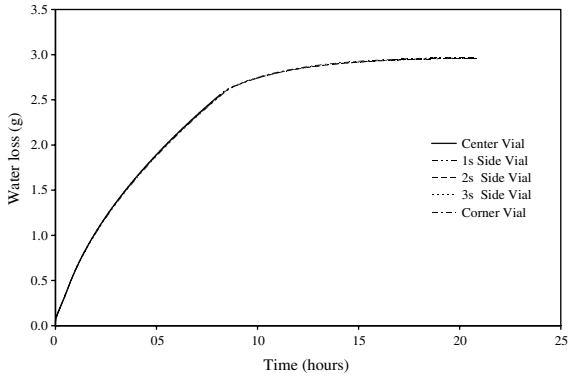

Fig. 8. Water loss as a function of time for the vials of case (b).

mention here that the results in Figs. 7–9 are supported by the experimental data of the systems studied by Kobayashi et al. [2].

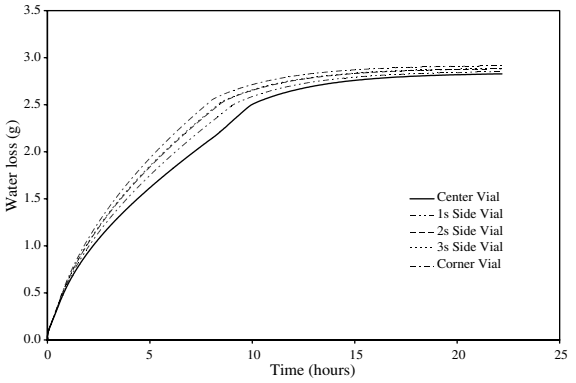

Fig. 9. Water loss as a function of time for the vials of case (c).

4. Conclusions and remarks

For all three lyophilization cases (a)–(c) studied in this work, fast drying times and relatively uniform distributions in the concentration of bound water at the end of the secondary drying stage were obtained by heat input control that runs the lyophilization process close to the melting and scorch temperature constraints. By comparing the results obtained for cases (a)–(c), it was found that case (b) where the trays have no tray sides and the drying chamber wall was kept at 263.15 K (i) yields the shortest overall drying time, (ii) provides the most uniform water loss among vials located at different positions on the tray, and (iii) produces a more uniform distribution of concentration of bound water in the product in the vials at the end of the secondary drying stage of the lyophilization process. The results of this work indicate that it would be beneficial to operate the lyophilization process of a product in vials by (1) employing freeze-dryers whose trays have no tray sides, (2) using heat input control that runs the lyophilization process close to the melting temperature constraint

during the primary drying stage and close to the scorch temperature constraint during the secondary drying stage, and (3) keeping the drying chamber wall temperature slightly higher than the melting temperature constraint during the primary drying stage, while during the secondary drying stage the drying chamber wall temperature should not be significantly lower than the scorch temperature constraint. Furthermore, the experimental observations of Kobayashi et al. [2] can be explained by the theoretical results obtained in this work and also the modeling and system formulation approach presented here provide a quantitative method that can be used in the analysis, optimization and control of the freeze-drying process, as well as in the design of freeze-dryers.

Finally, since it is very important to control the drying chamber wall temperature during the freezing stage [11–13] of the lyophilization process and the results of this work indicate that it would be desirable to keep the drying chamber wall temperature, in freeze-dryers using trays without tray sides, close to the melting and scorch temperature constraints during the primary and secondary drying stages, respectively, it seems appropriate that pilot-scale and industrial freeze-dryers should be constructed to have the capability to implement control of the drying chamber wall temperature.

Acknowledgement

The authors are grateful for the support of this work by Criofarma-Freeze Drying Equipment, Turin, Italy.

References

[1] F. Franks, Biophysics and Biochemistry at Low Temperature, Cambridge University Press, Cambridge, England, 1985.
[2] M. Kobayashi, K. Harashima, R. Sunama, A.R. Yao, Inter-vial variance of the sublimation rate in shelf freeze-dryer, Actes Congr. Int. Froid, 18th 4 (1991) 1711–1715.
[3] P. Sheehan, A.I. Liapis, Modeling of the primary and secondary drying stages of the freeze drying of pharmaceutical products in vials: numerical results obtained from the solution of a dynamic and spatially multi-dimensional lyophilization model for different operational policies, Biotechnol. Bioeng. 60 (1998) 712–728.
[4] L. Rey, J.C. May (Eds.), Freeze-Drying/Lyophilization of Pharmaceutical and Biological Products, Marcel Dekker, Inc., New York, NY, USA, 1999.
[5] O. Cornu, X. Banse, P.L. Docquier, S. Luyckx, C. Delloye, Effect of freeze drying and gamma irradiation on the mechanical properties of human cancellous bone, J. Orthop. Res. 18 (2000) 426–431.
[6] K.H. Gan, R. Bruttini, O.K. Crosser, A.I. Liapis, Heating policies during the primary and secondary drying stages of the lyophilization process in vials: effects of the arrangement of vials in clusters of square and hexagonal arrays on trays, Drying Technol. 22 (2004) 731–769.
[7] S. Kirkpatrick, Percolation and conduction, Rev. Mod. Phys. 45 (1973) 574–588.
[8] M. Sahimi, B.D. Hughes, L.E. Scriven, H.T. Davis, Real-space renormalization and effective-medium approximation to the percolation conduction problem, Phys. Rev. B 28 (1983) 307–311.
[9] J.H. Petropoulos, A.I. Liapis, N.P. Kolliopoulos, J.K. Petrou, N.K. Kanellopoulos, Restricted diffusion of molecules in porous affinity chromatography adsorbents, Bioseparation 1 (1990) 69–88.
[10] D. Stauffer, A. Aharony, Introduction to Percolation Theory, 2nd ed., Taylor and Francis, London, England, 1992.
[11] R. Bruttini, O.K. Crosser, A.I. Liapis, Exergy analysis for the freezing stage of the freeze drying process, Drying Technol. 19 (2001) 2303–2313.
[12] K.H. Gan, R. Bruttini, O.K. Crosser, A.I. Liapis, The effects of tray side and drying chamber wall temperature on the performance of freeze-drying in vials arranged in clusters of square and hexagonal arrays on trays for different heat input control policies, Paper V12 Presented at the Internal Meeting of the GVC-Technical Committee Drying Technology, jointly with the EFCE Working Party on Drying, Nuremberg, Germany, March 16–18, 2004.
[13] D. Gehrmann, Exploring the influence of the lyophilization system on the homogeneity of the freeze drying process, Paper V13 Presented at the Internal Meeting of the GVC-Technical Committee Drying Technology, jointly with the EFCE Working Party on Drying, Nuremberg, Germany, March 16–18, 2004.
[14] K.H. Gan, The dependence of the overall drying time and product quality of a lyophilization process on the relative position of vials on a tray with tray sides and without tray sides for different heat input control policies, Ph.D. thesis, University of Missouri-Rolla, Rolla, MO, 2004.
[15] ISO 8362-1 (E), Injection containers for injectables and accessories—Part 1: Injection vials made of glass tubing, 1989.
[16] A.I. Liapis, R. Bruttini, A theory for the primary and secondary drying stages of the freeze drying of pharmaceutical crystalline and amorphous solutes: comparison between experimental data and theory, Sep. Technol. 4 (1994) 144–155.